Review

Scalable solution processing of amorphous and crystalline chalcogenide films

Nikita S. Dutta[1] and Craig B. Arnold[1,*]

Chalcogenide materials have attracted interest for diverse device applications, including thermoelectrics, phase-change memory and optoelectronics, and even solid-state batteries. Part of their appeal is solution processability, which offers a potentially inexpensive, scalable route to thin film fabrication. A number of solution-based methods have been explored with crystalline metal chalcogenides, but combining industrially practical solvents with high-throughput film deposition remains challenging. Similar issues are faced with amorphous chalcogenides, where decades of work has focused on the role of dissolution chemistry in processing high-quality films. Here, we outline recent progress in understanding dissolution and film formation in both systems. By combining wisdom from crystalline and amorphous chalcogenides, we aim to highlight fundamentals underlying scalable solution processing and map areas for future study.

Combining wisdom from crystalline and amorphous chalcogenides

Chalcogenide materials have attracted interest for an ever-growing list of potential applications, from phase-change memory for neuromorphic computing [1,2], to solid electrolytes and electrodes for next-generation batteries [3,4], to thermoelectrics and topological materials [5,6]. Their breadth in properties of interest follows in part from diversity in the materials themselves; unified by inclusion of the chalcogens sulfur (S), selenium (Se), or tellurium (Te), chalcogenides can contain a wide array of other elements in structures ranging from 2D [7] to 3D, crystalline [8,9] to amorphous [10], or even combinations thereof [11]. Even as these varied subsystems have their own unique properties and considerations, there are many areas of overlap enabled by their similar chemistry. This is particularly true in thinking about solution processing, a common tool for fabricating thin films of chalcogenide glasses or crystalline metal chalcogenides. Here, the structures that separate crystalline and amorphous materials are broken down and rebuilt *en route* to the final thin film. Arsenic-sulfur (As-S) compounds, for instance, form similar nanostructures during dissolution whether starting from a glassy or crystalline bulk precursor [12,13]. Antimony-sulfur (Sb-S) compounds, meanwhile, form an amorphous phase on deposition that must be thermally transformed to the final crystal structure [14,15]. Solution processing thus blurs lines between these two classes of chalcogenides at both ends, from dissolution to film formation. This opens the door for productive exchange between the communities that study them.

In developing solution-based routes for amorphous and crystalline chalcogenide films alike, scalability is often of primary concern. Compared with vacuum-based methods [16,17], material deposition from solutions – or more broadly, 'inks' – is generally less expensive and more industrially practical. At times, this can come at the expense of film purity, so scalability gains must be significant enough to make solution processing worthwhile for device applications. To this end, significant advances have been made in recent years towards phasing out hazardous traditional solvents [18–21] and expanding to novel non-chalcogenide and elemental precursors that allow flexible and economical composition tailoring [22–24]. These are accompanied by improvements

Highlights

Chalcogenide materials are of interest for an ever-growing list of applications in optoelectronics, thermoelectrics, energy storage, and more.

Amines and amine mixtures have been shown to effectively process amorphous and crystalline chalcogenide films from a wide variety of precursors.

The solubility of elemental chalcogens and metals allows fine-tuning of chalcogenide composition through solution processing.

Annealing is essential to film formation, and protocols have been developed that lead to film quality on a par with vacuum-based deposition techniques.

Recent work has leveraged the properties imparted by impurities in the as-deposited film to fabricate solution-processed doped or nanostructured films.

[1]Department of Mechanical and Aerospace Engineering, Princeton Institute for the Science and Technology of Materials, Princeton University, Princeton, NJ 08544, USA

*Correspondence:
cbarnold@princeton.edu (C.B. Arnold).

in thermal post-processing to bring film quality on a par with that of vacuum deposition [9,25]. However, gaps in our understanding of ink chemistry and its effects on film formation remain, limiting our ability to fine-tune the phase, purity, and morphology of films through informed choice of processing parameters. In many cases, the fundamental nature of these open questions cross-cuts the amorphous and crystalline chalcogenide subfields.

In this review, we focus on combining wisdom from these adjacent systems on the chemistry at both ends of solution processing: dissolution and film formation. For the former, we highlight progress with amine solvents, which alone and in mixtures have come to take on a prominent role in solution processing of amorphous and crystalline chalcogenides alike. We describe their traditional uses in dissolving bulk chalcogenides and newer successes with diverse non-chalcogenide and elemental precursors. For all three, we review recent efforts to understand the underlying dissolution mechanisms. This leads to our subsequent discussion of film formation, where we review how the species present in inks undergo annealing-driven processes that determine the final material structure. Here, we highlight avenues to enhance phase purity as well as the benefits of retaining certain controlled impurities. By drawing connections between amorphous and crystalline systems at the front and back ends of solution processing, we bring attention to open questions in our fundamental understanding and highlight opportunities to develop new methods that further exploit the scalability of solution deposition.

Dissolution chemistry

Many early efforts to solution process chalcogenide materials used hydrazine, mainly due to its effectiveness as a solvent and ability to yield residue-free films [18–21,26]. Unfortunately, hydrazine is also extremely toxic and volatile, limiting the scalability of processing routes that rely on it. Thus, while hydrazine processing is still used [27,28], a huge amount of effort has been made to investigate more industrially friendly options. In recent years, relatively less hazardous solvents like ethanol [29,30], dimethylformamide (DMF) [30–35], butyldithiocarbamate acid (BDCA) [14,36–38], dimethylsulfoxide (DMSO) [32–34,39], and even water [33,40,41] have been explored. Among the various options, a particular spotlight has been placed on amines. Both alone and in solvent mixtures, amines have proved effective in the processing of chalcogenide thin films with a range of compositions and structures, offering interesting overlaps between crystalline and amorphous systems. In this section, we focus on amines, reviewing recent progress in understanding the dissolution of bulk chalcogenides and the doors opened by non-chalcogenide and elemental precursors. We also highlight opportunities for transferable progress between work on amorphous and crystalline systems.

Dissolution of bulk chalcogenides

Amines have long been used to solution process thin films from bulk chalcogenide glass precursors. Early work has established the viability of solvents like n-propylamine (PA) and ethylenediamine (EDA; also abbreviated as EN in other work) [12,42] with bulk As_2S_3 glass as a precursor, while recent attention has shifted to n-butylamine (BA) [43–45], ethanolamine (ETA) [25,46–48], and broader glass compositions [43–49]. Notably, initial studies of chalcogenide glasses in PA and EDA postulated that dissolution proceeds through the formation of solvent-dependent nanostructures [12,49,50] – 'clusters' in the former, shown in Figure 1, and 'branched chains' in the latter – which have recently been structurally characterized by cryoelectron microscopy [51]. Pioneering work on the formation of these structures is well summarized by previous reviews [52], but recent studies have grown our understanding. For As-S glasses in BA, for instance, Slang and colleagues have drawn attention to the importance of atomic bonding disorder in the bulk precursor, proposing a mechanism in which the solvent preferentially interacts with
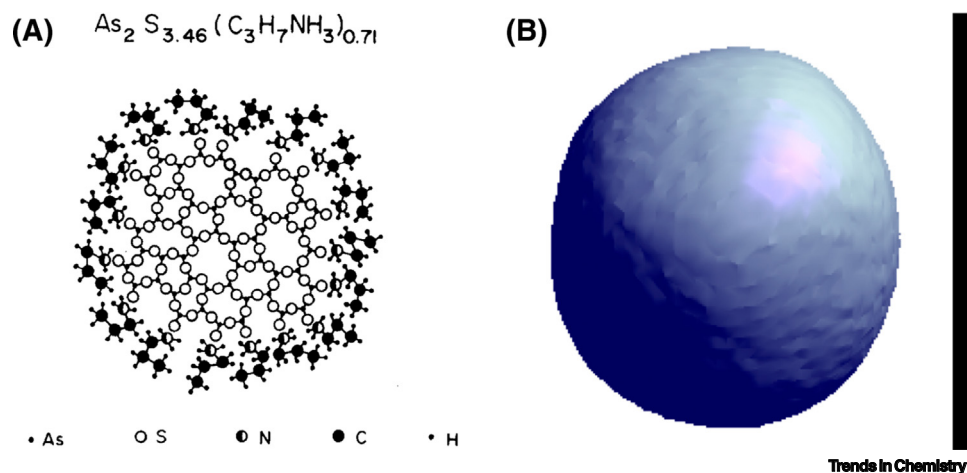
Figure 1. Bulk chalcogenide glasses form nanostructures in amines. (A) Cluster structure proposed for As_2S_3 in propylamine (PA). Reprinted from [50], with the permission of AIP Publishing. (B) 3D reconstruction of cluster produced by cryoelectron microscopy analysis of As_2S_3 in PA inks. Bar, 3 nm. Adapted, with permission, from [51].

homopolar S–S bonds to break the glass into clusters. Based on this, they suggest that the chalcogen content of the glass should influence both the dissolution rate and the size of clusters in the ink [43].

This argument delves deeper into the specifics of cluster-mediated dissolution than earlier theories that attribute cluster formation to a simple breaking of the layer-like structure that chalcogenide glasses tend to display [50,53]. Moreover, that the mechanism is predicated on the presence of disordered bonding supports observations that amines alone are inadequate to dissolve many crystalline chalcogenides and thus require solvent mixing [54,55], as is discussed shortly. However, certain complexities in the dissolution of bulk chalcogenide glasses remain to be understood. Crystalline As-S precursors still form clusters when dissolved in EDA [13] and the attribution of cluster size to homopolar bonding does not explain observations that cluster sizes in BA [56,57], PA [58], and EDA [13] depend on the concentration of chalcogenide in the ink, even for a fixed chalcogenide composition. The latter phenomenon has been proposed to relate instead to the equilibrium concentration of amine salt species that form during solvent–solute interaction and encapsulate the clusters [58]. These details point to the lack of an overarching theory to unite key parameters linked with cluster formation and demonstrate that despite the long history of processing films from amines and amorphous chalcogenide precursors, fundamental gaps in understanding of the dissolution chemistry remain.

These open questions have not prevented progress from being made in broadening amine processing to a wider range of bulk chalcogenide precursors. Recent work has used PA, ETA, and BA to process novel germanium (Ge)-based glass compositions [45,47–49], with Waldmann and colleagues proposing a cluster structure for germanium antimony sulfide ($Ge_{23}Sb_7S_{70}$) in PA [49]. As Ge-based glasses are increasingly popular due in part to their elimination of toxic As, this expansion enhances scalability yet again and broadens the range of commercially practical devices accessible through solution processing. Further gains have been made by the development of amine-based solvent mixtures. Webber and colleagues first demonstrated that a 1:10 volume mixture of ethanedithiol (EDT) in EDA dissolves a variety of V_2VI_3 chalcogenides – binary compounds of chalcogens and Group V elements [54]. Since then, this mixture has been used to dissolve additional precursors, including transition metal chalcogenides like copper sulfide

(Cu$_2$S) or copper selenide (Cu$_2$Se) [55,63,72], and broadened to other combinations of amines and thiols [65,73]. Table 1 shows how the already wide array of bulk chalcogenides processable in amines is expanded by solvent mixing. Importantly, amine-thiol mixtures are capable of yielding molecular solutions [54,74], unlike the unary amine inks described previously that contain nanostructures. Their solvating power has been ascribed to the formation of ionic RS$^-$ species in the mixture [54,55,65], marked by a large increase in ionic conductivity observed on combining the two solvents [54,65]. In a successful example of the combining of wisdom across chalcogenide subfields, adaptations to this cosolvent approach have shown that both 1:10 thiol-amine and methanol-amine mixtures enhance the solubility of Se-rich chalcogenide glasses, which have traditionally posed more of a dissolution challenge than their S-containing counterparts [68,75].

Non-chalcogenide and elemental precursors

To achieve films with more complex compositions, bulk chalcogenide precursors may be unavailable or financially impractical for industrial purposes. Consequently, a main strength of solvent mixtures with high solvating power has been in enabling the use of non-chalcogenide precursor compounds. Wang and colleagues showed how BA could be used as a starting material to process metal chalcogenide films from metal oxide precursors by reacting it with carbon disulfide (CS$_2$) to form BDCA [36]. Although not properly a solvent mixture, this represented an early example of the value of combining amines with a S source to diversify possible precursors. Later, McCarthy and colleagues demonstrated that crystalline metal sulfide films could be readily prepared from metal oxide precursors dissolved in thiol-amine mixtures, with the alkanethiol component of the solvent acting as the S source. Certain selenide films were also possible after adding Se to the metal oxide-based ink [22]. The versatility of precursors that have since been used with this kind of approach is well captured by previous reviews [74]; besides continued work with metal oxide precursors [9,63,76], metal chloride precursors have also been widely investigated in recent years [77–79]. While the introduction of unwanted elements through these routes offers less direct control of film composition, it can be a highly cost-effective choice for scalable film fabrication by enabling use of Earth-abundant metal sources.

Recently, elemental precursors have arisen as an exciting and desirable alternative to bulk chalcogenide and non-chalcogenide compounds alike. These have the benefit of maintaining the purity of the deposited chalcogenide, as no new elements are introduced during the process besides those in the solvent, while also offering greater compositional flexibility. The most readily soluble elemental chalcogen is S, and Palka and colleagues used its solubility in BA to process S-rich As-S glass films from a commercial As-S precursor and additional elemental S. Their

Table 1. Bulk chalcogenide precursors tested with common processing amines and amine-based mixtures[a]

|	PA	BA	HA	EDA	ETA
Unary (no mixing)	As-S [42]; As-Se* [59]; Ge-Sb-S [49]	As-S [50]; As-Se* [59]; As-S-Se [61]; Ge-Sb-S [45]	As-S [60]; Ge-Sb-S* [47]	As-S [50]; As-Se [59]	As-S, As-Se [25]; As-S-Se, As-S-Ge [46]; Ge-Sb-S [47]
EDT	Ag-S, Cu-S [62]	Ag-S, Ag-Se, Cu-S, Cu-Se, In-S, In-Se, Sn-S, Sn-Se [65]	Ag-S, Ag-Se, Cu-S, Cu-Se, In-S, In-Se Sn-S, Sn-Se [65]	Ag-S [63]; As-X, Bi-X [54]; Cu-S, Cu-Se, Fe-Se [64]; In-S, In-Se [66]; Sb-X [54]; Sn-S [67]	
Propanethiol	As-Se* [68]		Cu-Se*, In-Se* [69]		
Mercaptoethanol				As-S, As-Se [70]; Cu-S [71]; Sb-S, Sb-Se, Sn-S, Zn-S [70]	
Methanol	As-Se [68]				

[a]Columns correspond to amines, while rows correspond to mixing solvents. An X in the composition denotes that all three chalcogens (S, Se, and Te) have been tested. Asterisks indicate that the composition is tested in the cited work but does not yield good results.

results from Raman spectroscopy show a structure in $As_{30}S_{70}$ films processed from $As_{40}S_{60}$ and elemental S that is remarkably similar to those processed from bulk $As_{30}S_{70}$ [24]. This demonstrates an exciting new route to use solution processing to simply alter the composition of available precursors, rather than having to melt-quench a new glass. Elemental Se and Te, meanwhile, are soluble in thiol-amine mixtures [23,39,65,73,80,81], and the underlying mechanisms are being explored. Deshmukh and colleagues recently showed that the nature of solvated Se species depends on both the choice of amine and thiol and their mixing ratio, ranging from long-chain polyselenides in BA-ET with low thiol content to monoselenium thiolate in EDA-ET with excess thiol. This is depicted by the proposed reaction scheme in Figure 2 [73]. These results highlight how, like the cluster-containing inks described in the preceding text, the structures in inks prepared with elemental precursors depend on a combination of processing parameters.

Further compositional control – and with it, further complexity – arises with the solubility of elemental metals in thiol-amine mixtures [23,39,65]. This enables fine-tuning of ternary or quaternary alloys. Zhao and colleagues recently proposed a model for the dissolution of indium (In) in hexylamine (HA)-EDT, in which the elemental metal is oxidized to In^{3+} and coordinated with four S atoms in an exothermic reaction that releases hydrogen (H_2) gas. This elemental loss during gas release prevents reversal of the reaction on evaporation of the solvent mixture, allowing the researchers to redissolve the metal thiolate complexes in DMF, a less corrosive solvent, for deposition [39]. This innovation, illustrated in Figure 3, demonstrates how a deeper understanding of dissolution promotes improvement of the solution process as a whole. Besides allowing broader material compatibility during film fabrication, the formation of molecular complexes in thiol-amine mixtures paired with deposition from benign solvents can also be explored to overcome issues damaging lower layers during iterative spin coating of thick films [45,69].

Despite this progress, lingering gaps in our understanding of elemental chalcogen and metal dissolution impede full compositional tailoring with such precursors. For instance, certain elemental metals like Sb [80] or gallium (Ga) [23] are not readily soluble in thiol-amine mixtures in the absence of Se. This is in contrast to their soluble compounds like gallium trichloride ($GaCl_3$) [69] or antimony trioxide (Sb_2O_3) [22]. As a consequence, a combination of elements and non-chalcogenide compounds is often required to achieve the most comprehensive toolkit for the
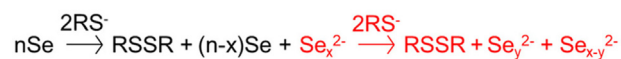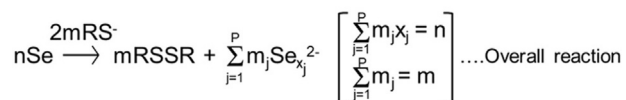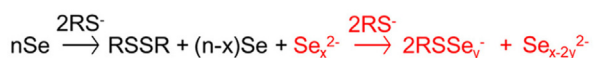
Figure 2. Proposed reaction scheme for dissolution of elemental Se. Schemes for Se in monoamine-monothiol (top) versus diamine-monothiol (bottom) mixtures depict the formation of polyselenides in the former and monoselenium thiolates ($RSSe^-$) in the latter. Reprinted with permission from [73]. Copyright 2020 American Chemical Society.

Monoamine-monothiol

$$nSe \xrightarrow{2mRS^-} mRSSR + \sum_{j=1}^{P} m_j Se_{x_j}^{2-} \begin{bmatrix} \sum_{j=1}^{P} m_j x_j = n \\ \sum_{j=1}^{P} m_j = m \end{bmatrix} ....\text{Overall reaction}$$

$$nSe \xrightarrow{2RS^-} RSSR + (n-x)Se + Se_x^{2-} \xrightarrow{2RS^-} RSSR + Se_y^{2-} + Se_{x-y}^{2-}$$

Diamine-monothiol

$$nSe \xrightarrow{2mRS^-} (m-n/2)RSSR + nRSSe^- \qquad ....\text{Overall reaction}$$

$$nSe \xrightarrow{2RS^-} RSSR + (n-x)Se + Se_x^{2-} \xrightarrow{2RS^-} 2RSSe_y^- + Se_{x-2y}^{2-}$$
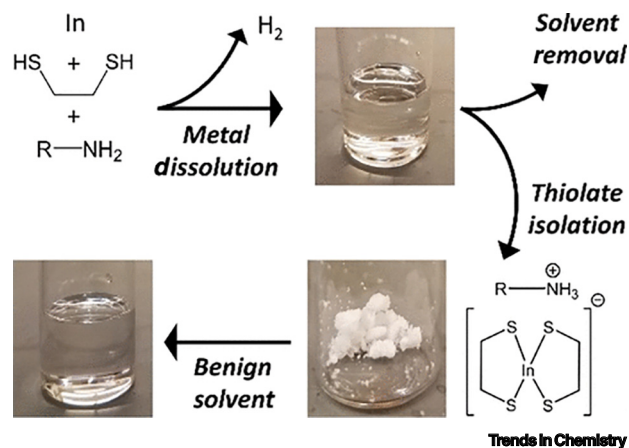
Trends in Chemistry

Figure 3. Opportunities with elemental metal precursors. Understanding dissolution mechanisms for elemental metals in thiol-amines enables new opportunities in solution processing. This diagram shows the formation of metal complexes in thiol-amines followed by redissolution in a benign solvent for deposition. Reprinted with permission from [39]. Copyright 2019 American Chemical Society.

tailoring of film composition, which comes at the potential expense of purity. Furthermore, the thermodynamic limits of solution-based composition alteration have not been fully characterized. Even in situations where the desired precursors are readily soluble, as in the processing of S-rich As-S glasses [24], questions remain on the limitations of phases accessible in the final material and the deposition conditions required to ensure phase homogeneity. Thus, to take full advantage of the flexibility of elemental precursors and fairly compare them with other processing methods, it is first necessary to better understand how the species present in inks affect film formation.

Film formation

A variety of deposition methods are used in solution processing of chalcogenide films [29,48,82], but film formation across these is united by the subsequent thermal and chemical conversion steps. With the range of complicated species and structures present in inks, described in the previous section, as-deposited films require at least annealing, if not sulfurization or selenization, to achieve the desired phase structure. The former refers to heat treatment alone, generally under inert atmosphere; note that while, in the glass community, 'annealing' implies the use of temperatures past a specific annealing point, here we use a broader definition of any heat treatment that allows structural relaxation, residual solvent removal, or both. The latter two treatments, meanwhile, involve heating under the respective chalcogen atmosphere to chemically alter the deposited material. In this section, we review recent work in understanding these two types of treatment and their effects on film formation, focusing more heavily on annealing as it is ubiquitous among amorphous and crystalline chalcogenides and more favored for scalability. In particular, we highlight how the processes that make annealing necessary can also lead to unwanted effects, and we discuss recent creative work that turns film impurity into opportunity.

Thermal conversion and annealing

Some solution processing routes yield chalcogenide films directly, without the need for chemical conversion of the as-deposited phase. The most straightforward example of this is found in chalcogenide glass films processed from bulk chalcogenide precursors. Here, amorphous chalcogenide films form immediately on deposition, traditionally through spin coating [42,43,50,56,82–85], although recent work has also focused on other methods, such as electrospray [47,48] or doctor-blading [29]. Direct formation of an amorphous phase also occurs in the processing of certain metal chalcogenide films, with annealing required to reach the desired crystal structure. This is particularly common with metal V_2VI_3 chalcogenides like Sb_2S_3 [14,15], although it has also been

observed with broader compositions [63,65,79,86]. While these routes are convenient due to the lack of sulfurization or selenization steps, the as-deposited phase suffers from low purity and suboptimal morphology. Amines, in particular, leave behind carbon, nitrogen, and hydrogen residues [87] and nanostructures in inks can propagate into the dried material [56]. Thus, even in films intended to remain glassy, annealing is required to remove residual solvent or precursors and improve the material structure.

Annealing time and temperature play significant roles in film quality for both crystalline and amorphous chalcogenides [9,59,61,82,87,88]. Recent work has shown that the structural and optical properties of chalcogenide glass films are more influenced by annealing temperature than the amine aliphatic chain length [60]. This is notable given the influence of solvent choice on cluster formation, although comparisons with diamines have shown certain solvent-dependent optical properties even after annealing [89]. Importantly, annealing is capable of bringing certain measures of film quality on a par with those produced by high-purity vacuum techniques. Prince and colleagues showed that annealing glassy As-S and As-Se films spin coated from ETA at sufficiently high temperature (150°C) increased the refractive index to that of a thermally evaporated film and the electrical conductivity beyond it [25]. This echoed earlier work that showed such property improvements to be related to residual solvent removal [87]. Embden and colleagues also demonstrated that optimal annealing of solution-processed $CuSbS_2$ absorber layers for solar cells yielded power conversion efficiencies above 1% and on a par with earlier work using sputtering [9,90]. These findings are critical to making solution processing truly practical for device applications.

The thermochemical processes that occur during annealing, however, can also bring about unwanted effects. Zhao and colleagues showed that hot-plate annealing of $Cu(In,Ga)Se_2$ precursor films before selenization led to significant Ga loss when metal chlorides were used to prepare the original thiol-amine ink. They postulated this was due to the formation of $GaCl_3$, whose boiling point (150°C) was lower than the annealing temperatures used (250–350°C) [69]. Similarly, Strizik and colleagues observed the formation of voids in PA-processed As_3S_7 films on annealing at 200 and 300°C, shown in Figure 4, due to the evaporation of H_2S gas formed as a consequence of residual solvent [82,91]. Importantly, both studies were able to combat these film-formation effects by altering ink preparation. For Zhao and colleagues, non-chloride precursors produced films with up to 86% higher Ga content [69], while Strizik and colleagues observed that the addition of tris(8-hydroxyquinolinato)erbium(III) complex (ErQ) eliminated damage during annealing, as seen in Figure 4 [82]. These results highlight the intimate link between ink preparation and film formation. Further optimization of post-deposition thermal processing must begin with a deeper understanding of complexes present in inks to predict thermochemical reactions in the as-deposited films.

Chemical conversion

A significant drawback to metal chalcogenide processing is that films often require an additional annealing under chalcogen atmosphere to reach the desired phase purity [23,30,40,69,72,86]. These sulfurization or selenization steps detract from the overall scalability of the process. While S sources added during ink preparation like thiols [65], thiourea [34], or CS_2 [9] have been sufficient to eliminate the need for sulfurization, selenization remains common to control film Se content even when depositing from inks with Se sources [23,69,72]. As this is largely to replace S with Se in films targeting Se-rich final compositions, this once again brings attention back to ink preparation and the possibility of reducing S contamination by limiting S sources. The low solubility of Se makes this a tall order [80,81], but the aforementioned case of adopting thiol-amine processing for chalcogenide glasses may provide some insight. Although Slang and
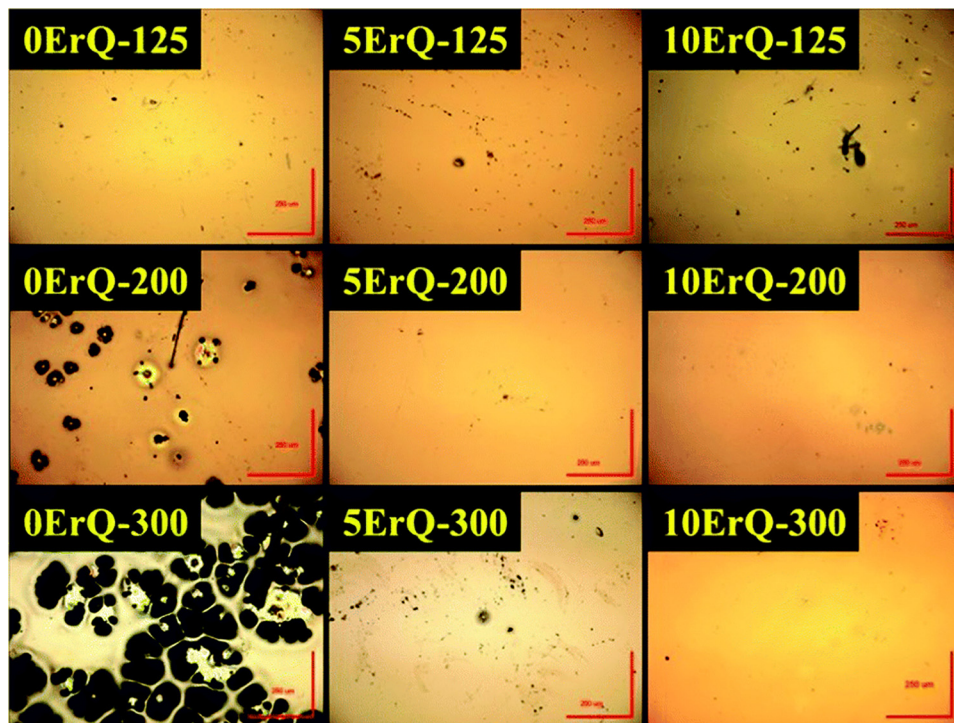
Trends in Chemistry

Figure 4. Interplay of ink preparation and annealing. Defects form in As_3S_7 films as the annealing temperature is increased from 125°C to 200°C to 300°C (left side, top to bottom). The introduction of 5 or 10 mol% tris(8-hydroxyquinolinato)erbium(III) complex (ErQ) precursor, relative to the bulk As_3S_7 precursor, mitigates the damage (left to right), demonstrating the relationship between ink preparation and annealing. Bars (red), 250 μm. Reproduced, with permission, from [82].

colleagues observed that a thiol-amine mixture dissolved the bulk As-Se precursor, as described previously, the deposited films showed low optical quality, which they suggested to be related to S contamination. Replacing the thiol with methanol, however, both dissolved the precursor and yielded a film with the desired Se content and high optical quality [68]. While amorphous and crystalline chalcogenides are subject to different processing challenges, this example demonstrates how continuous exchange of ideas between the two subfields stands to deepen our understanding of film formation and generate valuable new ideas.

Benefits of non-chalcogenide residues

Even as these routine thermal and chemical treatments attempt to enhance the purity of the deposited chalcogenide phase, it is critical to recognize that not all residues are undesirable. Nanoparticle- or ion-doped chalcogenide glass films, for instance, exploit controlled impurities for applications across photonics, but fabricating them often requires laser processing [17,83,85] or prefabricated quantum dots [92,93]. This detracts from the convenient solution processability of the glasses themselves. Single-step doping, meanwhile, relies on the dissolution of additional precursors in the ink to form the dopant *in situ*, which remains as a 'residue' in the film – a simpler, more scalable alternative. The addition of silver chloride (AgCl) or ErQ to PA-based inks has been successfully used to solution process Ag_2S- or Er^+-doped As-S films, respectively [82,84,94]. These demonstrate the potential of the method but deal with a small selection of dopants relative to what has been accomplished with other techniques [85,92,93]. This represents an opportunity for advances in the identification of elemental and non-chalcogenide precursors for metal

chalcogenide films, detailed in the preceding text, to be extended to amorphous systems. Particularly as metal chalcogenide nanocrystals themselves are viable dopants for chalcogenide glass films [84,92–94], an interesting avenue for future work would be to explore the potential of the diverse solvent–precursor pairings investigated by the crystalline chalcogenide community to expand the variety of dopants possible with single-step solution processing of glassy films.

Further opportunities to use the presence of unwanted ink components in as-deposited films in advantageous ways have focused on solvent residues. Tzadka and colleagues recently demonstrated a method for direct nanoimprinting of glassy As_2Se_3 films processed from EDA by leveraging the plasticizing effect of residual solvent, shown in Figure 5A,B [95]. Around the same time, Wang and colleagues observed that metal-organic precursors formed during BDCA processing could act as negative resists during lithography. As shown in Figure 5C, they used this to pattern the as-deposited film with an electron beam before annealing to form the desired metal chalcogenide phase [38]. A key advantage of studies like these is that they go beyond simply seeking compositional control of solution-processed chalcogenide films to explore interesting benefits of impurities that arise along the way. Thus, alongside continued work to improve film formation and post-processing, a promising direction for future study is to consider nontraditional applications of the unique properties imparted by residual solvent or precursors to develop new processes that leverage the speed and scalability of solution deposition.

Concluding remarks

Growing interest in next-generation applications of chalcogenides in recent years has fortunately been accompanied by significant advances in scalable solution processing of chalcogenide thin films. The already vast array of bulk chalcogenides soluble in amines has been augmented by explorations of amine-based solvent mixtures, and recent successes with elemental precursors have opened new doors to facile composition tailoring. These not only are paired with informed

Outstanding questions

How do processing parameters interplay to control the formation of nanoscale clusters or molecular complexes in inks prepared with bulk chalcogenide, non-chalcogenide, or elemental precursors?

What are the thermodynamic limitations of composition tailoring through elemental precursors?

What solvent systems are capable of processing Se-rich compositions with minimal S contamination?

Can the diversity of precursors explored to fabricate metal chalcogenide films be applied to single-step doping of chalcogenide glass films?

How can impurities imparted during solution processing be leveraged for creative device applications?
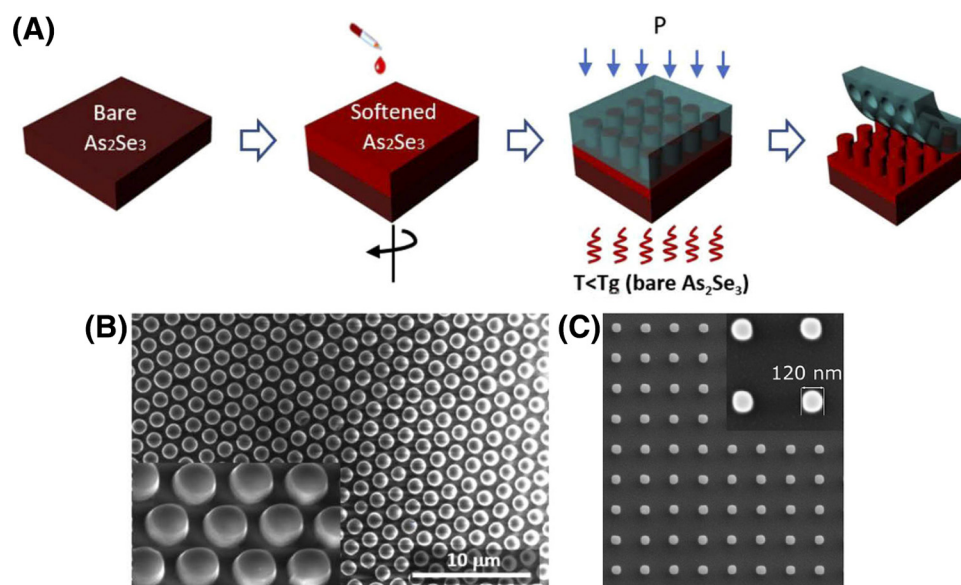
Trends in Chemistry

Figure 5. Applications of impurities in as-deposited films for patterning. (A) Schematic of nanoimprinting using plasticizing effect of residual solvent in deposited film and (B) example antireflective pattern imprinted onto As_2Se_3 film. Adapted, with permission, from [95]. (C) Example Sb_2S_3 dot pattern produced by lithography of as-deposited film. Adapted, with permission, from [38].

thermal processing to produce films on a par with vacuum-based deposition methods, but have also been leveraged to fabricate more complex doped or nanostructured films. Still, these advances make it apparent that, whether considering a nanostructured ink for a chalcogenide glass or a molecular ink for a metal chalcogenide, the reactive nature of the solvent is of paramount importance. Work remains to fully understand the dissolution mechanisms, whose chemical nature means that parameters like precursor or solvent choice, solvent mixing ratio, and precursor concentration directly influence the nature of the solvated species (see Outstanding questions). These, in turn, determine the processes that occur during film formation, including annealing-driven reactions that significantly impact the quality of the final material.

To expand the reach of scalable solution processing to new devices on the horizon for chalcogenide materials, from neuromorphic synapses [1] to wearable thermoelectrics [5,96], future work should target open questions on these fundamentals of dissolution and film formation. Understanding the structures present in inks more deeply is essential to enable more rigorous control of the deposited phase, particularly when seeking to produce Se-rich films or to push the limits of composition tailoring with elemental precursors. Alongside this, future work should continue to investigate novel applications of the diverse precursors already characterized and the interesting impurities that arise in the early stages of film formation. In these endeavors, helpful insights can be found by combining wisdom on amorphous and crystalline systems, enabling a more foundational understanding of the solution process as a whole and promoting more rapid development of chalcogenide film fabrication to keep pace with the ever-evolving applications.

Declaration of interests

The authors declare no interests.

References

1. Xu, M. *et al.* (2020) Recent advances on neuromorphic devices based on chalcogenide phase-change materials. *Adv. Funct. Mater.* 30, 2003419
2. Aryana, K. *et al.* (2021) Interface controlled thermal resistances of ultra-thin chalcogenide-based phase change memory devices. *Nat. Commun.* 12, 774
3. Hayashi, A. *et al.* (2019) A sodium-ion sulfide solid electrolyte with unprecedented conductivity at room temperature. *Nat. Commun.* 10, 5266
4. Aslam, M.K. *et al.* (2020) Metal chalcogenide hollow polar bipyramid prisms as efficient sulfur hosts for Na-S batteries. *Nat. Commun.* 11, 5242
5. Ren, W. *et al.* (2021) High-performance wearable thermoelectric generator with self-healing, recycling, and Lego-like reconfiguring capabilities. *Sci. Adv.* 7, eabe0586
6. Krishnamoorthy, H.N.S. *et al.* (2020) Infrared dielectric metamaterials from high refractive index chalcogenides. *Nat. Commun.* 11, 1692
7. Manzeli, S. *et al.* (2017) 2D transition metal dichalcogenides. *Nat. Rev. Mater.* 2, 17033
8. Han, J. *et al.* (2020) Solution-processed Sb_2S_3 planar thin film solar cells with a conversion efficiency of 6.9% at an open circuit voltage of 0.7 V achieved via surface passivation by a $SbCl_3$ interface layer. *ACS Appl. Mater. Interfaces* 12, 4970–4979
9. van Embden, J. *et al.* (2020) Solution-processed $CuSbS_2$ thin films and superstrate solar cells with CdS/In_2S_3 buffer layers. *ACS Appl. Energy Mater.* 3, 7885–7895
10. Lepicard, A. (2018) Demonstration of dimensional control and stabilization of second harmonic electro-optical response in chalcogenide glasses. *Opt. Mater. Exp.* 8, 1613–1624
11. Song, X. *et al.* (2019) Soft chemical synthesis of H_xCrS_2: an antiferromagnetic material with alternating amorphous and crystalline layers. *J. Am. Chem. Soc.* 141, 15634–15640
12. Guiton, T.A. *et al.* (1989) Solution/gelation of arsenic trisulfide in amine solvents. *Chem. Mater.* 1, 558–563
13. Wang, J. *et al.* (2008) Arsenic(II) sulfide quantum dots prepared by a wet process from its bulk. *J. Am. Chem. Soc.* 130, 11596–11597
14. Wang, X. *et al.* (2017) A fast chemical approach towards Sb_2S_3 film with a large grain size for high-performance planar heterojunction solar cells. *Nanoscale* 9, 3386–3390
15. Kondrotas, R. *et al.* (2018) Sb_2S_3 solar cells. *Joule* 2, 857–858
16. Riha, S.C. *et al.* (2017) Low-temperature atomic layer deposition of $CuSbS_2$ for thin-film photovoltaics. *ACS Appl. Mater. Interfaces* 9, 4667–4673
17. Normani, S. *et al.* (2020) Comparative study of Er^{3+}-doped Ga-Ge-Sb-S thin films fabricated by sputtering and pulsed laser deposition. *Sci. Rep.* 10, 7997
18. Mitzi, D.B. *et al.* (2004) High-mobility ultrathin semiconducting films prepared by spin coating. *Nature* 428, 299–303
19. Mitzi, D.B. *et al.* (2005) Low-voltage transistor employing a high-mobility spin-coated chalcogenide semiconductor. *Adv. Mater.* 17, 1285–1289
20. Milliron, D.J. *et al.* (2006) Solution-processed metal chalcogenide films for p-type transistors. *Chem. Mater.* 18, 587–590
21. Milliron, D.J. *et al.* (2007) Solution-phase deposition and nano patterning of GeSbSe phase-change materials. *Nat. Mater.* 6, 352–356
22. McCarthy, C.L. *et al.* (2015) Solution-phase conversion of bulk metal oxides to metal chalcogenides using a simple thiol-amine solvent mixture. *Angew. Chem. Int. Ed.* 54, 8378–8381

23. Zhao, D. *et al.* (2015) Solution-deposited pure selenide CIGSe solar cells from elemental Cu, In, Ga, and Se. *J. Mater. Chem. A* 3, 19263–19267

24. Palka, K. *et al.* (2019) Modification of solution processed thin chalcogenide films composition by source solution doping. *J. Non-Cryst. Solids* 517, 76–82

25. Prince *et al.* (2017) Electrical and optical properties of solution phase deposited As$_2$S$_3$ and As$_2$Se$_3$ chalcogenide thin films: a comparative study with thermally deposited films. *J. Non-Cryst. Solids* 476, 46–51

26. Romanyuk, Y.E. *et al.* (2015) All solution-processed chalcogenide solar cells – from single functional layers towards a 13.8% efficient CIGS device. *Adv. Funct. Mater.* 25, 12–27

27. Zhou, Y. *et al.* (2014) Solution-processed antimony selenide heterojunction solar cells. *Adv. Energy Mater.* 4, 1301846

28. Yang, B. *et al.* (2015) Hydrazine solution processed Sb$_2$S$_3$, Sb$_2$Se$_3$ and Sb$_2$(S$_{1-x}$Se$_x$)$_3$ film: molecular precursor identification, film fabrication and band gap tuning. *Sci. Rep.* 5, 10978

29. Rukcharoen, N. *et al.* (2019) Effect of low thermal treatment temperatures on the morphological, optical and electrical properties of Sn$_{1-x}$Mn$_x$Te nanocomposite films incorporated with indium cations. *Ceram. Int.* 45, 23203-2315

30. Yan, R. *et al.* (2018) Solution-processed Cu$_2$ZnSnS$_4$ thin film with mixed solvent and its application in superstate structure solar cells. *RSC Adv.* 8, 11469–11477

31. Choi, Y.C. *et al.* (2015) Efficient Sb$_2$S$_3$-sensitized solar cells via single-step deposition of Sb$_2$S$_3$ using S/Sb-ratio-controlled SbCl$_3$-thiourea complex solution. *Adv. Funct. Mater.* 25, 2892–2898

32. Kwon, S.M. *et al.* (2018) High-performance and scalable metal-chalcogenide semiconductors and devices via chalco-gel routes. *Sci. Adv.* 4, eaap9104

33. Wu, C. *et al.* (2020) Water additive enhanced solution processing of alloy Sb$_2$(S$_{1-x}$Se$_x$)$_3$-based solar cells. *Sol. RRL* 4, 1900582

34. Maiti, A. *et al.* (2020) Sulfur-vacancy passivation in solution-processed Sb$_2$S$_3$ thin films: influence on photovoltaic interfaces. *ACS Appl. Energy Mater.* 3, 810–821

35. Nie, R. *et al.* (2020) Heteroleptic tin-antimony sulfoiodide for stable and lead-free solar cells. *Matter* 3, 1701–1713

36. Wang, G. *et al.* (2012) A novel and versatile strategy to prepare metal–organic molecular precursor solutions and its application in Cu(In,Ga)(S,Se)$_2$ solar cells. *Chem. Mater.* 24, 3993–3997

37. Lui, Y. *et al.* (2019) Butyldithiocarbamate acid solution processing: its fundamentals and applications in chalcogenide thin film solar cells. *J. Mater. Chem. C* 7, 11068–11084

38. Wang, W. *et al.* (2020) Direct patterning of metal chalcogenide semiconductor materials. *Adv. Funct. Mater.* 30, 2002685

39. Zhao, X. *et al.* (2019) Investigating chemistry of metal dissolution in amine-thiol mixtures and exploiting it toward benign ink formulation for metal chalcogenide thin films. *Chem. Mater.* 31, 5674–5682

40. Prabhakar, R.R. *et al.* (2016) Photovoltaic effect in earth abundant solution processed Cu$_2$MnSnS$_4$ and Cu$_2$MnSn(S,Se)$_4$ thin films. *Sol. Energy Mater. Sol. Cells* 157, 867–873

41. Whyte, G.M. *et al.* (2020) Optical and photoluminescence performance of electrode posited arsenic selenide thin film doped with erbium ion. *Opt. Mater.* 99, 109556

42. Chern, G.C. *et al.* (1982) Spin coated amorphous chalcogenide films. *J. Appl. Phys.* 53, 6979–6982

43. Slang, S. *et al.* (2015) Mechanism of the dissolution of As–S chalcogenide glass in *n*-butylamine and its influence on the structure of spin coated layers. *J. Non-Cryst. Solids* 426, 125–131

44. Márquez, E. *et al.* (2017) Optical characterization of amine-solution-processed amorphous AsS$_2$ chalcogenide thin films by the use of transmission spectroscopy. *J. Alloys Compd.* 721, 363–373

45. Slang, S. *et al.* (2019) Solution processed Ge$_{20}$Sb$_5$S$_{75}$ thin films: the effect of solution concentration and multiple layers stacking. *Opt. Mater. Exp.* 9, 4360–4369

46. Prince, S.R. *et al.* (2015) Solution based approach for the fabrication of photonic devices in chalcogenide glasses. *AIP Conf. Proc.* 1665, 070021

47. Novak, S. *et al.* (2015) Deposition of Ge$_{23}$Sb$_7$S$_{70}$ chalcogenide glass films by electrospray. *Thin Solid Films* 588, 56–60

48. Novak, S. (2017) Direct electrospray printing of gradient refractive index chalcogenide glass films. *Appl. Mater. Interfaces* 9, 26990–26995

49. Waldmann, M. *et al.* (2012) Structural properties of solution processed Ge$_{23}$Sb$_7$S$_{70}$ glass materials. *J. Mater. Chem.* 22, 17848–17852

50. Chern, G.C. *et al.* (1983) Spin coated amorphous chalcogenide films: structural characterization. *J. Appl. Phys.* 54, 2701–2705

51. Dutta, N.S. *et al.* (2020) Understanding solution processing of inorganic materials using cryo-EM. *Opt. Mater. Exp.* 10, 119–128

52. Zha, Y. *et al.* (2013) A review on solution processing of chalcogenide glasses for optical components. *Opt. Mater. Exp.* 3, 1259–1272

53. Leadbetter, A.J. *et al.* (1974) Diffraction studies of glass structure (V). The structure of some arsenic chalcogenide glasses. *J. Non-Cryst. Solids* 15, 250–268

54. Webber, D.H. *et al.* (2013) Alkahest for V$_2$VI$_3$ chalcogenides: dissolution of nine bulk semiconductors in a diamine-dithiol solvent mixture. *J. Am. Chem. Soc.* 135, 15722–15725

55. Lin, Z. *et al.* (2015) Cosolvent approach for solution-processable electronic thin films. *ACS Nano* 9, 4398–4405

56. Kohoutek, T. *et al.* (2008) Effect of cluster size of chalcogenide glass nanocolloidal solutions on the surface morphology of spin- coated amorphous films. *J. Appl. Phys.* 103, 1–6

57. Sebastian, I. *et al.* (2013) Concentration tuned bandgap and corresponding nonlinear refractive index dispersion in Ga-Ge-Se nanocolloids. *J. Appl. Phys.* 114, 053102

58. Dutta, N.S. *et al.* (2018) Concentration dependence of As$_2$S$_3$ chalcogenide glass cluster size in amine solution. *RSC Adv.* 8, 35819–35823

59. Zou, Y. *et al.* (2012) Effect of annealing conditions on the physiochemical properties of spin-coated As$_2$Se$_3$ chalcogenide glass films. *Opt. Mater. Exp.* 2, 1723–1732

60. Jancalek, J. *et al.* (2020) Comparison of solution processed As$_{33}$S$_{67}$ thin films deposited using primary amines of various aliphatic chain length. *J. Non-Cryst. Solids* 550, 120382

61. Kohoutek, T. *et al.* (2006) Spin-coated As$_{33}$S$_{67-x}$Se$_x$ thin films: the effect of annealing on structure and optical properties. *J. Non-Cryst. Solids* 352, 1563–1566

62. Deshmukh, S.D. *et al.* (2019) Versatile colloidal syntheses of metal chalcogenide nanoparticles from elemental precursors using amine-thiol chemistry. *Chem. Mater.* 31, 9087–9097

63. Ma, Y. *et al.* (2016) Thermoelectric properties of copper chalcogenide alloys deposited via the solution-phase using a thiol-amine solvent mixture. *RSC Adv.* 6, 99905–99913

64. Liu, F. *et al.* (2015) Low temperature, solution-deposited metal chalcogenide films as highly efficient counter electrodes for sensitized solar cells. *J. Mater. Chem. A* 3, 6315–6323

65. Zhang, R. *et al.* (2016) Metal–metal chalcogenide molecular precursors to binary, ternary, and quaternary metal chalcogenide thin films for electronic devices. *Chem. Commun.* 52, 5007–5010

66. Arnou, P. *et al.* (2015) Solution-processed CuIn(S,Se)$_2$ absorber layers for application in thin film solar cells. *Thin Solid Films* 582, 31–34

67. Antunez, P.D. *et al.* (2014) Low temperature solution-phase deposition of SnS thin films. *Chem. Mater.* 26, 5444–5446

68. Slang, S. (2018) Solution processed As$_{30}$S$_{70}$ chalcogenide glass thin films with specular optical quality: multi-component solvent approach. *J. Non-Cryst. Solids* 8, 948–959

69. Zhao, X. *et al.* (2016) Solution-processed sulfur depleted Cu(In,Ga)Se$_2$ solar cells synthesized from a monoamine-dithiol solvent mixture. *J. Mater. Chem. A* 4, 7390–7397

70. Buckley, J.J. *et al.* (2014) Ligand exchange of colloidal CdSe nanocrystals with stibanates derived from Sb$_2$S$_3$ dissolved in a thiol-amine mixture. *Chem. Mater.* 26, 6311–6317

71. McCarthy, C.L. *et al.* (2016) Earth abundant CuSbS$_2$ thin films solution processed from thiol-amine mixtures. *J. Mater. Chem. C* 4, 6230–6233

72. Arnou, P. *et al.* (2017) Solution processing of CuIn(S,Se)$_2$ and Cu (In,Ga)(S,Se)$_2$ thin film solar cells using metal chalcogenide precursors. *Thin Solid Films* 633, 76–80

73. Deshmukh, S.D. *et al.* (2020) Analyzing and tuning the chalcogen-amine-thiol complexes for tailoring of chalcogenide syntheses. *Inorg. Chem.* 59, 8240–8250

74. McCarthy, C.L. *et al.* (2017) Solution processing of chalcogenide materials using thiol-amine "alkahest" solvent systems. *Chem. Commun.* 53, 4888–4902

75. Slang, S. *et al.* (2020) Deposition and characterization of solution processed Se-rich Ge-Se thin films with specular optical quality using multi-component solvent approach. *Opt. Mater. Exp.* 10, 2973–2986

76. Wright, L.D. *et al.* (2019) Water based spray pyrolysis of metal-oxide solutions for $Cu_2ZnSn(S,Se)_4$ solar cells using low toxicity amine/thiol complexants. *Thin Solid Films* 669, 588–594

77. Zhang, R. *et al.* (2015) A versatile solution route to efficient $Cu_2ZnSn(S,Se)_4$ thin-film solar cells. *Chem. Mater.* 27, 2114–2120

78. Miskin, C.K. *et al.* (2016) A direct solution deposition approach to CdTe thin films. *J. Mater. Chem. C* 4, 9167–9171

79. Murria, P. *et al.* (2017) Speciation of CuCl and $CuCl_2$ thiol-amine solutions and characterization of resulting films: implications for semiconductor device fabrication. *Inorg. Chem.* 56, 14396–14407

80. Webber, D.H. *et al.* (2014) Facile dissolution of selenium and tellurium in a thiol-amine solvent mixture under ambient conditions. *Chem. Sci.* 5, 2398–2502

81. Walker, B.C. *et al.* (2014) Contamination-free solutions of selenium in amines for nanoparticle synthesis. *Chem. Commun.* 50, 8331–8334

82. Strizik, L. *et al.* (2017) Solution-processed Er^{3+}-doped As_3S_7 chalcogenide films: optical properties and 1.5 μm photoluminescence activated by thermal treatment. *J. Mater. Chem. C* 5, 8489–8497

83. Lu, C. *et al.* (2014) Fabrication of uniformly dispersed nanoparticle-doped chalcogenide glass. *Appl. Phys. Lett.* 105, 1–4

84. Almeida, J.M.P. *et al.* (2015) Single-step synthesis of silver sulfide nanocrystals in arsenic trisulfide. *Opt. Mater. Exp.* 5, 1815–1821

85. Gu, T. *et al.* (2017) Anisotropic crystallization in solution processed chalcogenide thin film by linearly polarized laser. *Adv. Phys.* 110, 041904

86. Madhusudanan, S.P. *et al.* (2021) Photoactive Cu_2FeSnS_4. *Appl. Surf. Sci.* 535, 147600

87. Song, S. *et al.* (2010) Influence of annealing conditions on the optical and structural properties of spin-coated As_2S_3 chalcogenide glass thin films. *Opt. Exp.* 18, 5472–5480

88. Slang, S. *et al.* (2017) Influence of annealing on the optical properties, structure, photosensitivity and chemical stability of $As_{30}S_{70}$ spin-coated thin films. *J. Non-Cryst. Solids* 457, 135–140

89. Dutta, N.S. *et al.* (2020) Effects of disorder on two-photon absorption in amorphous semiconductors. *Opt. Lett.* 45, 3228–3231

90. Welch, A.W. *et al.* (2016) Accelerated development of $CuSbS_2$ thin film photovoltaic device prototypes. *Prog. Photovolt. Res. Appl.* 24, 929–939

91. Zha, Y. *et al.* (2013) Pore formation and removal in solution-processed amorphous arsenic sulfide films. *J. Non-Cryst. Solids* 369, 11–16

92. Li, C. *et al.* (2017) Electrospray deposition of quantum dot-doped $Ge_{23}Sb_7S_{70}$ chalcogenide glass films. *Thin Solid Films* 626, 194–199

93. Slang, S. *et al.* (2017) Exposure enhanced photoluminescence of $CdS_{0.9}Se_{0.1}$ quantum dots embedded in spin-coated $Ge_{25}S_{75}$ thin films. *RSC Adv.* 7, 53830–53838

94. Almeida, J.M.P. *et al.* (2017) Nonlinear optical waveguides in As_2S_3-Ag_2S chalcogenide glass thin films. *Sci. Rep.* 7, 93–99

95. Tzadka, S. *et al.* (2020) Surface plasticizing of chalcogenide glasses: a route for direct nanoimprint with multifunctional antireflective and highly hydrophobic structures. *Opt. Exp.* 28, 28352–28365

96. Ju, H. *et al.* (2018) Solution-processable flexible thermoelectric composite films based on conductive polymer/$SnSe_{0.8}S_{0.2}$ nanosheets/carbon nanotubes for wearable electronic applications. *J. Mater. Chem. A* 6, 5627–5634